Journal of Molecular Graphics and Modelling 54 (2014) 100–106

Contents lists available at ScienceDirect

Journal of Molecular Graphics and Modelling

journal homepage: www.elsevier.com/locate/JMGM

# Investigation of the rescue mechanism catalyzed by a nucleophile mutant of rice BGlu1

Jinhu Wang[a,b], Rui Zhang[b], Rutao Liu[b,*], Yongjun Liu[c]

[a] College of Chemistry Chemical Engineering and Material Science, Zaozhuang University, Zaozhuang, Shandong 277160, China
[b] School of Environmental Science and Engineering, Shandong University, 27 Shanda South Road, Jinan 250100, China
[c] School of Chemistry and Chemical Engineering, Shandong University, Jinan, Shandong 250100, China

ARTICLE INFO

*Article history:*
Accepted 8 October 2014
Available online 22 October 2014

*Keywords:*
Rescue mechanism
β-Glucosidase
E386G mutant
Anionic formate
Anomeric carbon
Quantum mechanical/molecular mechanical (QM/MM)

ABSTRACT

In the present study, the quantum mechanical/molecular mechanical (QM/MM) method was used to investigate the rescue mechanism of an E386G mutant as well as the glycosylation mechanism of the wild rice β-D-glucosidase. E386G mutant experiences an asynchronous collaborative process to glycosylate the anionic formate with an energy barrier of 22.6 kcal/mol, while the energy barrier is 25.9 kcal/mol for the wild complex. The low energy barrier of the mutated complex suggests that anionic formate might be a good nucleophile to attack the anomeric carbon atom. Both energy barriers can be lowered when the leaving departure releases from the active site, suggesting that the product release, rather than chemistry, contributes to the rate limiting in BGlu1 mutants. Structure analyses also indicate that the external nucleophile has little steric hindrance with pocket residues and adjusts freely to proceed the rescue mechanism of the mutated complex. Our calculations provide a guide for the selectivity of exogenous nucleophiles in the future study of β-glucosidase.



## 1. Introduction

The glycoside hydrolase family 1 β-D-glucosidase from rice (BGlu1, systematically named Os3BGlu7) has been expressed in *Escherichia coli* [1] and exists widely in rice organs with high level of activities, such as tissues, flower and seeding shoot [2–6]. As a most well-studied plant enzyme, it is more efficiently to hydrolyze the β-(1,4)- and short β-(1,3)-linked glucooligosaccharides [7].

Rice BGlu1 has a pair of catalytic glutamate residues serving as the acid/base and nucleophile in the active site, respectively [8]. The catalytic groups are the carboxylic acid of these key residues, with the reaction proceeding via a covalent glycosyl–enzyme intermediate. The glycosylation and deglycosylation steps of this mechanism have been studied extensively by the quantum mechanical/molecular mechanical (QM/MM) method [9,10]. Mutations of β-glucosidase at catalytic glutamate residue in which the carboxylate nucleophile is replaced by a nonnucleophilic residue make the hydrolytic activity decrease to a very low level. The mutated glycoside hydrolase becomes a hydrolytically inactive enzyme, which is unable to form the glycosyl enzyme intermediate. However, this kind of enzyme is characteristic of the glycosynthase when glycosyl fluorides and suitable glycosyl acceptors are present [11,12]. Nonnucleophilic mutations of rice BGlu1 nucleophile E386(Glycine, alanine, and serine) have been generated and the E386G mutant, acting as glycosynthase, catalyzed the most rapid accumulation of transglycosylation products [13]. Recently, the crystal of E386G mutant has been obtained by Pengthaisong et al. [14] and we have studied the oligosaccharide synthesis mechanism of this mutant by a theoretical method [15]. Although hydrolytic activities of these mutants have lost, the glycosidic bond-cleaving catalytic activity could be rescued by the anionic nucleophile (such as formate) [13,16]. The exogenous nucleophile formate fits into the space created by removal of the carboxylate of mutant enzyme and function as external nucleophile. Hommalai et al. [13] proposes a rescue mechanism catalyzed by an exogenous nucleophile of rice BGlu1: the acid/base residue firstly protonates the glycosidic oxygen, then the anionic nucleophile formate functions the role of the old nucleophile E386 attacking the anomeric carbon (Fig. 1). But the rescue mechanism has not been reported in detail yet.

In this paper, we reported the QM/MM studies on the rescue mechanism of E386G mutant of rice β-glucosidase. The crystal structure is selected from the crystal structure obtained by Pengthaisong et al. [14] (PDB ID:3SCO). Since the substrate with a good leaving group (para-nitrophenyl, *p*NP) is favored for the formation of glycosyl-enzyme intermediate [17], substrates with a *p*NP

* Corresponding author. Tel.: +86 531 88364868; fax: +86 531 88364868.
*E-mail address:* rutaoliu@sdu.edu.cn (R. Liu).

http://dx.doi.org/10.1016/j.jmgm.2014.10.003
1093-3263/

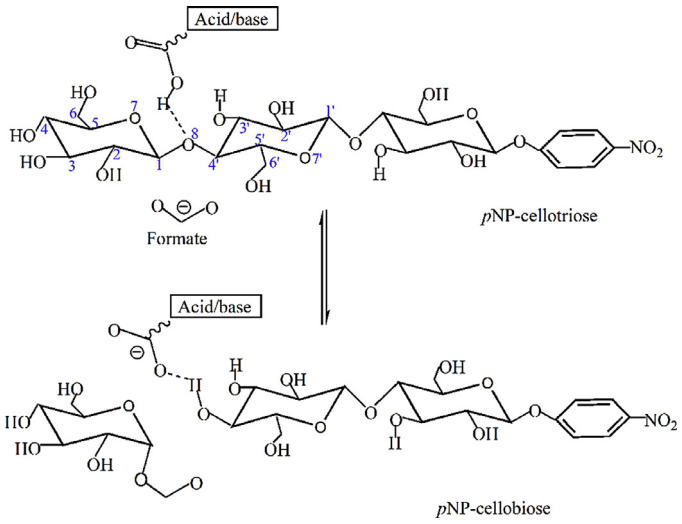


**Fig. 1.** Proposed rescue mechanism for the rice β-glucosidases.

moiety (such as *p*NP-β-cellobioside; *p*NP-β-cellotrioside, *p*NP-β-D-glucopyranoside and so on) is widely used in crystallization. In this study, the *p*NP-cellotriose was chosen as the substrate. The combined QM/MM method was applied to investigate how the external nucleophile formate influenced the catalytic mechanism of the mutant, which was expected to achieve a better description of catalytic mechanism. Since the surrogate mechanism leaves the glycosylated part of the substrate bound to the formate with likely no path to deglycosylating, this is not a study of the complete hydrolysis reaction. But the glycosylation step is the rate-limiting step, so it does not reduce the importance and impact of this investigation. Besides, in order to compare the difference between the mutated and wild complexes, the catalytic mechanism of the wild complex is also explored.

## 2. Computational methods

### 2.1. Automated docking setup

Computational models were constructed based on a X-ray crystal structure of rice BGlu1 E386G mutant (PDB ID: 3SCO). According to the experiment literature of Chuenchor et al. [7], the acid residue of rice BGlu1 was E176. So, all the glutamate residues except E176 were charged in the following molecular dynamics (MD) simulations. Using the docking approach in the Autodock 4.0 program [18], a grid box around the carboxylate side chain of E386 was created, and the formate group was docked into this space. The ligand *p*NP-cellotriose was firstly docked into the pocket and the anionic formate was then docked into the binary complex of the ligand with the protein. When docking, a grid box of 70 Å × 70 Å × 70 Å with a spacing of 0.375 Å was selected for *p*NP-cellotriose, and a grid box of 10 Å × 10 Å × 10 Å with a spacing of 0.375 was selected for formate. Gasteiger charges [19] were set for both ligands and protein. Fifty independent docking runs were performed. During the docking, the protein was kept rigid, and all the torsional bonds of the ligand were kept free. Based on a root-mean-square deviation (RMSD) criterion of 10 Å, the docking conformations were clustered. Finally, the conformation with the most cluster members and the lowest protein–ligand interaction energy was chosen as the bioactive structure for the investigation of the rescue mechanism.

Based on the docking structure of E386G–*p*NP–cellotriose–formate ternary complex, the external nucleophile formate was removed from the active site, then E386G mutation was mutated back to glutamate to generate a functional active site using Modeler 9.11 program [20–22]. A crystal structure of with E386 unchanged (PDB ID: 3F5L) was used as the template to decide the possible rotamer of the E386. A wild type rice BGlu1 complexed *p*NP-cellotriose was obtained, which was also used to explore catalytic mechanism.

### 2.2. QM/MM calculations

MD simulations were performed based on the obtained docking structure of E386G–*p*NP–cellotriose–formate ternary complex as well as the wild rice BGlu1 complexed *p*NP-cellotriose. All the glutamate residues except the acid/base E176 were charged and E176 was modeled in its protonated state, acting as a proton donor to the substrate. The protonation/deprotonation states of other ionizable residues were altered based on PROPKA method [23,24]. QM calculations were performed at the B3LYP/6-31G(d,p) level to achieve the Mulliken charge parameters of the substrates. All the hydrogen atoms were added with the HBUILD facility of the CHARMM package [25]. Extra 4762 water molecules were used to solvate the system, which generates a semidiameter of 38.1 Å water sphere for each system. To neutralize the system, nine $Cl^-$ ions were added at random for each system. A 1 ns MD simulation was carried out with the CHARMM22 forcefield [26] in order to equilibrate the prepared systems. For E386G system, the QM region included residues E176, Y315, G386, E440, the nucleophile formate and *p*NP-cellotriose, while for the wild structure, the QM region included residues E176, Y315, E386, E440, and *p*NP-cellotriose. The remaining part of each system was set as the MM region. During the QM/MM calculations, the QM region was treated by quantum mechanics under the Turbomole module [27] and the MM part by molecular mechanics under the CHARMM22 forcefield using the DL-POLY program [28]. QM/MM optimizations were performed at the B3LYP/6-31G(d,p)//CHARMM22 level. The electrostatic interactions between the QM and MM regions were treated by the standard electronic embedding scheme [29]. The covalent bonds across the QM/MM boundary was simulated by the charge shift model with hydrogen linked atoms [30]. The ChemShell package [31], incorporating the Turbomole and DL-POLY programs, were used to carry out QM/MM calculations. A geometry optimizer of hybrid delocalized internal coordinates (HDLC) [32] was adopted for the geometry optimizations. Stationary points were searched by the quasi-Newton limited memory Broyden–Fletcher–Goldfarb–Shanno (L-BFGS) algorithm [33,34], and transition states with the algorithm of partitioned rational function optimization (P-RFO) [35,36]. High level single point (SP) electronic energy calculations at a larger basis set of 6-31++G(d,p) were carried out to obtain accurate energies.

## 3. Results and discussion

### 3.1. Analyses of the substrate binding of docking and crystal structures

An overlap of the docking structure with the E386G mutant (Fig. 2a) and E176Q mutant (Fig. 2b) [37] was established to validate the reasonability of the binding mode of *p*NP-cellotriose and nucleophile formate, respectively. Fig. 2a gives the superposition of the docking structure with the corresponding crystal structure of E386G mutant (PDB ID: 3SCO). Two hydrogen bridges are formed between the side chain of E440 and two hydroxyl groups (at C4 and C6 atoms) of *p*NP-cellotriose with distances of 1.80 and 1.71 Å in the docking structure, respectively. The distance between the side chain of acid/base residue E176 and glycosidic oxygen is 2.90 Å, indicating E176 could donate its proton to the glycosidic oxygen in the following reaction. The terminal sugar ring of *p*NP-cellotriose

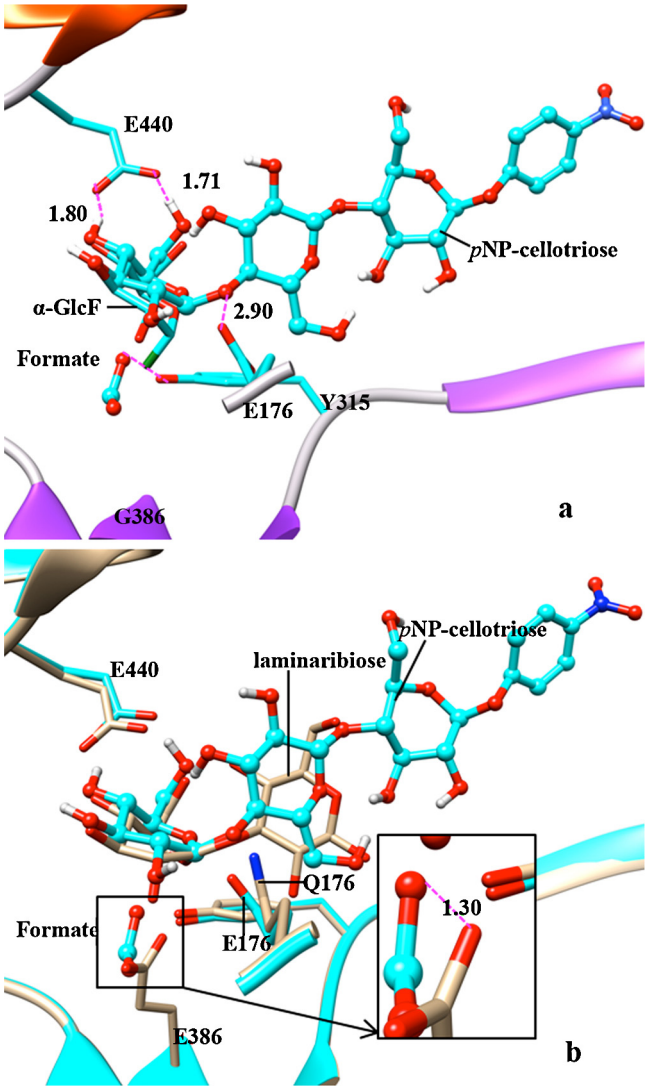


**Fig. 2.** An overlap of the docking structure with the corresponding crystal structure: (a) for E386G mutant (PDB ID: 3SCO); (b) for E176Q mutant (PDB ID: 3F5L).

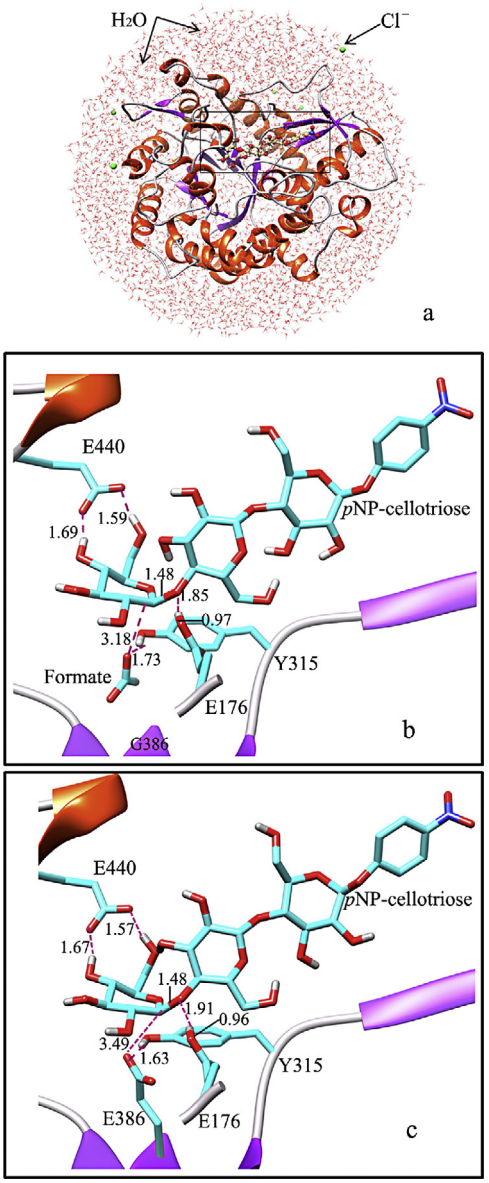


**Fig. 3.** (a) The structure of model system treated by CHARMM package; (b) pocket residues interactions in the active site of mutated complex; (c) pocket residues interactions in the active site of wild complex.

superposes well with the α-glucosyl fluoride (α-GlcF) in the crystal structure. Besides, the position of nucleophile formate is checked by the comparison of the docking structure with the crystal E176Q mutant, as shown in Fig. 2b. The superposition indicates that the nucleophile formate is located just at the side of the carboxyl group. All these descriptions indicate that the docking structure is reliable for the following QM/MM calculations.

### 3.2. Analyses of QM/MM calculation results

The solvent model constructed by CHARMM package is given in Fig. 3a and important interactions of the pocket residues with the substrate *p*NP-cellotriose for the mutated (E386G) and wild complexes are given in Fig. 3b and c. In the mutated complex, since the nucleophilic base E386 has been changed to G386, the nucleophile formate ($HCOO^-$) occupies the space where the base residue lies. So, the anionic formate functions the role of E386. Fig. 3b shows that the formate forms a hydrogen bond (HB) with the OH group of Y315 with a distance of 1.73 Å, where in the wild complex E386 also forms a HB with Y315 with a distance of 1.63 Å (Fig. 3c). The exist of this HB may contribute considerably to the stabilization of formate or E386. Though the base E386 and the external nucleophile formate all have carboxylate groups, the formate has more freedom to adjust its orientation to approach the anomeric carbon (C1, labeled in Fig. 1) than that of E386 in wild complex. It shows that the distance between the carboxylate group of the formate and C1 of *p*NP-cellotriose is 3.18 Å in E386G mutant, where it is 3.49 Å in the wild complex. Remote distances in the mutated and wild complexes reveal that the nucleophile group might have weak interactions with the ligand.

Besides, the side chain of the acid/base residue E176 forms a strong HB with the glycosidic oxygen (O8) in the mutated and wild complexes. The side chain of residue E440 is hydrogen bonded to hydroxyl groups at C4 and C6 positions in each structure. It assume that these HB interactions play a vital role in the following reactions.

Structures of reactant (**R**), transition state (**TS**), and product (**P**) were searched using B3LYP/6-31G(d,p)//CHARMM22 geometrical optimization in an adiabatic mapping procedure [38]. We scanned the reaction path along the reaction coordinates, where the saddle and stationary points were obtained. Definitions of the scanning variables and schematic showing of energy pathway scanning for mutated and wild complexes are given in Fig. S1 and S2. The saddle

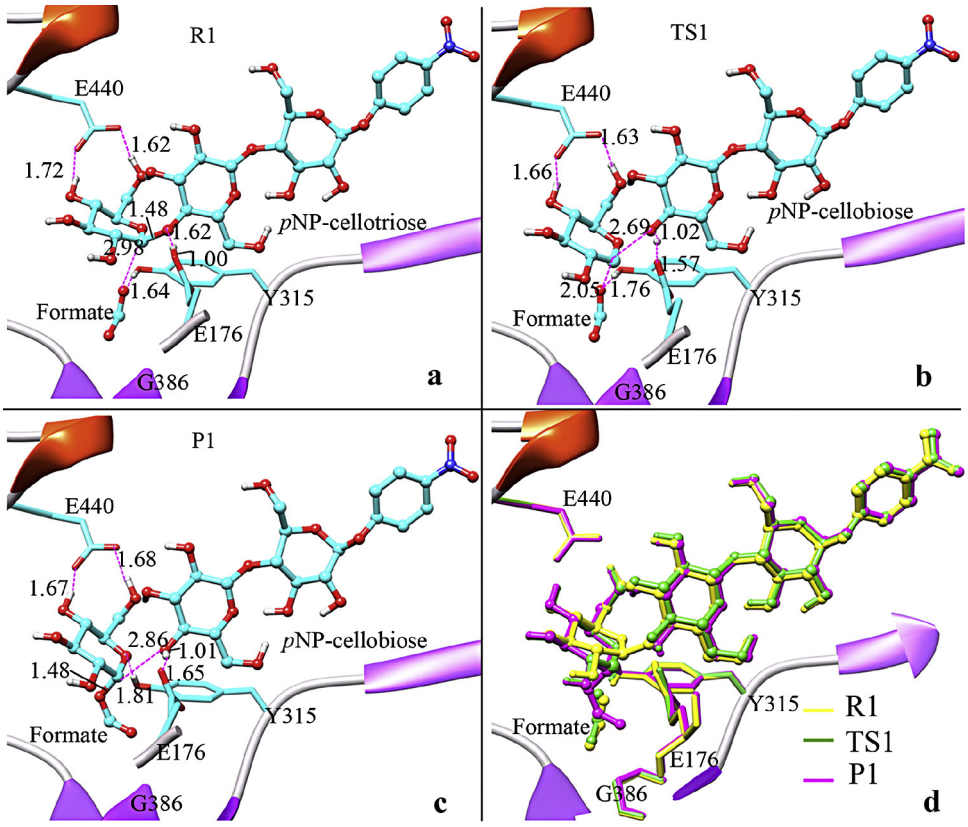


**Fig. 4.** Optimized geometries of reactant (**R1**), transition state (**TS1**), product (**P1**) and the superposition of active site residues in **R1**, **TS1** and **P1** for the mutated complex.

and stationary points were then optimized to be **TS** and **P** at the same level.

The structures of **R**, **TS**, and **P** for the mutated and wild complexes were optimized using QM/MM method, as shown in Figs. 4 and 5.

Reactants of **R1** and **R2** are given in Figs. 4a and 5a, respectively. The length of glycosidic bond (C1-O8) changes slightly in each structure: the bond length is 1.48 Å in **R1** and 1.46 Å in **R2**. Besides, the O8 atom establishes a strong HB with the carboxylate group of acid/base E176 with a length of 1.62 Å in **R1** and 1.70 Å in **R2**. Two hydrogen bridges are formed between E440 of the mutated complex and two hydroxyl groups (at C4 and C6 atoms) of *p*NP-cellotriose with distances of 1.72 and 1.62 Å, respectively, while in the wild complex, these HBs are 1.86 Å and 1.85 Å. Brás et al. proposed that these HB interactions contributed considerably to the stabilization of structures in the following reaction [39]. Since there is little steric hindrance between the exogenous nucleophile formate and G386, the anionic nucleophile can adjust its orientation to approach the C1 position: the distance changes from 3.18 Å in **R2** to 2.98 Å in **R1**. It means that the anionic formate might be a better nucleophile for the reaction. Furthermore, residue Y315 also forms a HB with the carboxylate group of nucleophile (formate or E386) in the mutated or wild complex with distances of 1.64 and 1.66 Å, respectively, indicating the important role of Y315 in reaction.

In **TS1** (Fig. 4b), acid E176 has almost donated its proton to O8 atom (distance of 1.02 Å), making the old H—O bond length of E176 increase to 1.57 Å. With the approach of E176 proton to O8 atom, the C1—O8 bond is almost broken with a bond length increasing to 2.69 Å. At the same time, the carboxylate group of the nucleophile formate approaches to the anomeric C1, the distance of which decreases to 2.05 Å. Obviously, formate has not been attached to C1. Overall, the last nucleophilic attack process proceeds in an asynchronous collaborative manner along with two previous processes of the protonation and glycosidic bond breaking. The HB formed between formate and Y315 in **R1** still exists in **TS1** (distance of 1.76 Å), which is thought to be favorable for the stability of the anionic nucleophile. Furthermore, hydrogen bridge interactions between E440 and two hydroxyl groups (C4 and C6 atoms) of *p*NP-cellotriose are also favored for the stabilities of TS. Brás et al. [39] believed that the role of these HB interactions was to lower the energy barrier, which was favorable for the formation of TS. In **TS2** of the wild complex (Fig. 5b), the formation and breakage ways of the bonds are similar to that of **TS1**. Difference lies in that some bonds become weakened during the bond cleavage. For example, the distance between the nucleophile E386 and C1 atom is 2.20 Å, while this length is 2.05 Å in **TS1**. Besides, residues Y315 and E440 also weaken their HBs with the hydroxyl groups of *p*NP-cellotriose.

For **P1** (Fig. 4c), E176 has transferred its proton to O8 atom with the formation of new H—O bond (length of 1.01 Å). During the proton transfer process, the old C1—O8 has broken completely (distance of 2.86 Å) and the carboxylate oxygen of the nucleophile formate has been attached to C1 atom of terminal saccharide residue (length of 1.48 Å). It shows that the leaving group (*p*NP-cellobiose) has departed after the attachment of formate to C1 atom. However, HBs formed between formate and Y315 in **R1** and **TS1** have disappeared in **P1**, and a new HB is formed between O7 atom and Y315 (distance of 1.81 Å). Y315 contributes to the stability of the terminal saccharide residue by forming a HB with the sugar ring, while it contributes to the stability of the nucleophile formate in **R1** and **TS1** by the formation of a HB with the oxygen atom of formate. Also, interactions of the hydrogen bridges formed between E440 and two hydroxyl groups (at positions of C4 and C6) of *p*NP-cellotriose still exist, lengths of which change to 1.67 and 1.68 Å, respectively. The product of the wild complex (**P2**) is shown in Fig. 5c. Though the C1 atom has attached to the carboxylate group

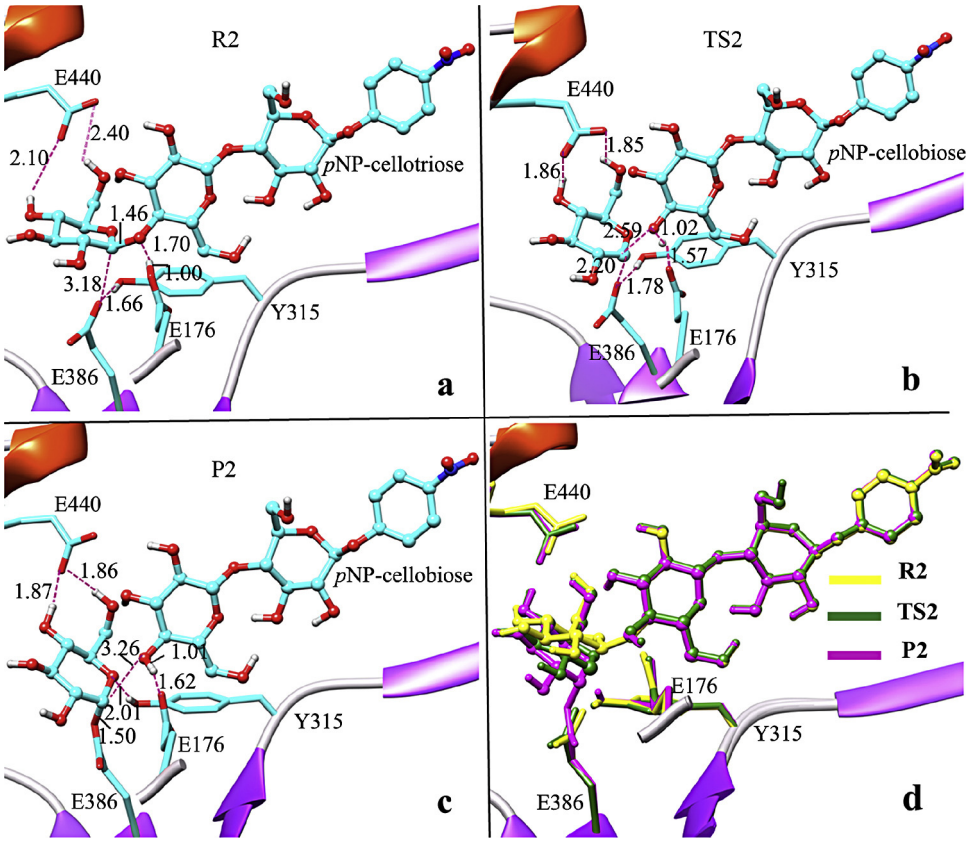


**Fig. 5.** Optimized geometries of **R2**, **TS2**, **P2** and the superposition of active site residues in **R2**, **TS2** and **P2** for the wild complex.

of E386, the newly formed covalent bond is a little weak (1.50 Å). As a residue of the enzyme, E386 might have less freedom than formate and cannot freely adjust its orientation to accept the sugar ring. So, the glycosidic bond has been elongated to 3.26 Å in **P2**, which is 0.40 Å longer than that of **P1**.

The superposition of active site residues in **R1**, **TS1** and **P1** is shown in Fig. 4d, where the superposition of **R2**, **TS2** and **P2** is given in Fig. 5d. Two Figures indicate that the initial conformation of C1 atom of *p*NP-cellotriose is reversed after the reaction, in which the conformation of C1 changes from *S* to *R* type, similar to previous study [9,10]. Analyses of the superpositions of nucleophiles (formate and E386) in two systems reveal that orientations of nucleophiles change slightly in the reactants and transition states, but adjust largely in the products. Furthermore, the rotation angle of formate is relatively larger than that of E386. This is because that anionic formate is an external nucleophile and has little steric hindrance with the pocket residue. So, nucleophile formate has more freedom than E386 and can adopt an optimal orientation to accept the sugar ring.

Energies of the optimized structure were recalculated with SP calculations using 6-31++G(d, p) basis set. The relative energies of the mutated and wild complexes are shown in Fig. 6. It shows that the activation barrier is only 22.6 kcal/mol for the E386G mutant, while it is 25.9 kcal/mol for the wild complex. Since in our QM/MM calculations the protein motion was not included in the search for the transition state, the activation barrier is relatively high, especially for the wild complex. Precise thermodynamic equilibrium study might solve this problem. The wild enzyme probably does rearrange at least somewhat in its product and perhaps transition state leading to lower energy than calculated here after thermodynamic study. However, it is not possible to do such kind of QM calculations and search configurational space of the

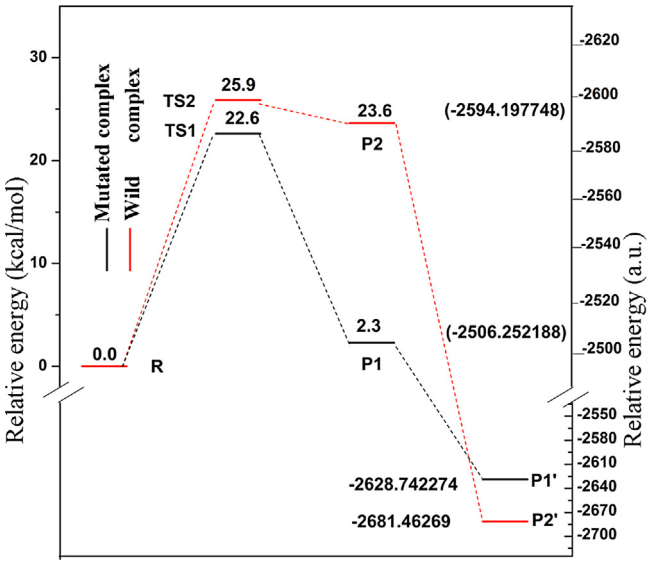


**Fig. 6.** Energy profile of the rescue and glycosylation mechanisms.

protein. Above all, the present results indicate that in the mutated complex the nucleophile formate might be a good nucleophile to attack the anomeric C1 atom. Besides, the product in the wild enzyme has a 23.6 kcal/mol uphill. The barrier of reverse reaction (Product → Transition state → Reactant) is calculated to be just 2.3 kcal/mol (compared with a 25.9 kcal/mol barrier to glycosylation). It seems that the hydrolytic activity of the wild enzyme is inactivated compared with the glycosynthesis of the reverse reaction. Yet, the wild enzyme has the hydrolysis function and it

does actually perform hydrolysis on glycosidic bonds in the natural world. The higher energy barrier of the uphill might be due to the difficulty of product release. Al though the rate limiting step in these mutants has not been established, Shoham has suggested that product release is likely a rate limiting step in glycosynthases [40]. Considering the size of the product and the nature of the active site, it is likely that the product release, rather than chemistry, is rate limiting in BGlu1 mutants. In order to investigate the influence of the product release, we performed QM/MM calculations to simulate the product without the leaving departure in the QM region. Optimized structures of **P1′** (Fig. S3a) and **P2′** (Fig. S3b) correspond to product without considering the leaving departure in the pocket, where the corresponding energies are also listed in Fig. 6. It shows that the energy of the product **P2′** becomes rather low comparing with the previous **P2**, indicating that the release of the leaving departure is favored for the proceeding of the glycosylation.

## 4. Conclusions

In this study, the rescue mechanism of an E386G mutant in complex with *p*NP-cellotriose and nucleophile formate was compared with the normal glycosylation step in the wild complex. The glycosylated part of the substrate experiences a surrogate mechanism to bound with the anionic formate with likely no path to deglycosylate in the next step, so it is only a halve study of the complete hydrolysis reaction. Calculations reveal that even in the mutated complex the proton attack of E176 on glycosidic oxygen and nucleophile attack of the anionic formate on anomeric C1 are an asynchronous collaborative process. Structural analyses indicate that the anionic nucleophile formate adopts a different way to interact with C1 atom. Comparing with the nucleophile E386, the external nucleophile has little steric hindrance with the pocket residue. It rotates slightly in **R1** and **TS1**, and changes largely in **P1**. The rescue mechanism of the mutated complex experiences an energy barrier of 22.6 kcal/mol, while the energy barrier for the wild complex is 25.9 kcal/mol. The high energy barrier can be lowered when the leaving departure releases from the active site, showing that the product release, rather than chemistry, contributes to the rate limiting in BGlu1 mutants. The low energy barrier of mutated complex suggests that formate might be a good nucleophile. Our calculations may provide a guide for the selectivity of exogenous nucleophiles in the future study of β-glucosidase.

## Acknowledgements

This work is supported by NSFC (20875055, 21277081, 21477067), the Cultivation Fund of the Key Scientific and Technical Innovation Project, Research Fund for the Doctoral Program of Higher Education, Ministry of Education of China (708058, 20130131110016), the Natural Science Foundation of China Postdoctoral Sustentation (2013M531603), Postdoctoral Innovation Project Special Funds of Shandong Province (201303109), Research Award Fund for Outstanding Young Scientists of Shandong Province (BS2013SW037), National Science Foundation for Young Scientists of China (31100584).

## Appendix A. Supplementary data

Supplementary data associated with this article can be found, in the online version, at http://dx.doi.org/10.1016/j.jmgm.2014.10.003.

## References

[1] R. Opassiri, J.R. Ketudat Cairns, T. Akiyama, O. Wara-Aswapati, J. Svasti, A. Esen, Characterization of a rice β-glucosidase highly expressed in flower and germinating shoot, Plant Sci. 165 (2003) 627–638.
[2] B. Henrissat, A classification of glycosyl hydrolases based on amino acid sequence similarities, Biochem. J. 280 (1991) 309–316.
[3] R. Opassiri, J.R. Ketudat Cairns, T. Akiyama, O. Wara-Aswapati, J. Svasti, A. Esen, Plant regeneration from soybean cotyledonary node segments in culture, Plant Sci. 165 (2003) 627–638.
[4] R. Opassiri, Y. Hua, O. Wara-Aswapati, T. Akiyama, J. Svasti, A. Esen, C.J.R. Ketudat, Beta-glucosidase, exo-beta-glucanase and pyridoxine transglucosylase activities of rice BGlu1, Biochem. J. 379 (2004) 125–131.
[5] W. Chuenchor, S. Pengthaisong, J. Yuvaniyama, R. Opassiri, J. Svasti, J.R.K. Cairns, Purification, crystallization and preliminary X-ray analysis of rice BGlu1-glucosidase with and without 2-deoxy-2-fluoro-D-glucoside, Acta Crystallogr. Sect. F: Struct. Biol. Cryst. Commun. 62 (2006) 798–801.
[6] W. Chuenchor, S. Pengthaisong, R.C. Robinson, J. Yuvaniyama, W. Oonanant, D.R. Bevan, A. Esen, C.J. Chen, R. Opassiri, J. Svasti, J.R.K. Cairns, Structural insights into rice BGlu1 beta-glucosidase oligosaccharide hydrolysis and transglycosylation, J. Mol. Biol. 377 (2008) 1200–1215.
[7] W. Chuenchor, S. Pengthaisong, R.C. Robinson, J. Yuvaniyama, J. Svasti, J.R. Cairns, The structural basis of oligosaccharide binding by rice BGlu1 beta-glucosidase, J. Struct. Biol. 173 (2011) 169–179.
[8] B. Henrissat, I. Callebaut, S. Fabrega, P. Lehn, J.P. Mornon, G. Davies, Conserved catalytic machinery and the prediction of a common fold for several families of glycosyl hydrolases, Proc. Natl. Acad. Sci. USA 92 (1995) 7090–7094.
[9] J.H. Wang, Q.Q. Hou, L.H. Dong, Y.J. Liu, C.B. Liu, QM/MM studies on the glycosylation mechanism of rice BGlu1 beta-glucosidase, J. Mol. Graph. Model. 30 (2011) 148–152.
[10] J.H. Wang, Q.Q. Hou, X. Sheng, J. Gao, Y.J. Liu, C.B. Liu, Theoretical study on the deglycosylation mechanism of rice BGlu1 beta-glucosidase, Int. J. Quantum Chem. 113 (2013) 1071–1075.
[11] S.J. Williams, S.G. Withers, Glycosynthases: mutant glycosidases for glycoside synthesis, Aust. J. Chem. 55 (2002) 3–12.
[12] G. Perugino, B. Cobucci-Ponzano, M. Rossi, M. Moracci, Recent advances in the oligosaccharide synthesis promoted by catalytically engineered glycosidases, Adv. Synth. Catal. 347 (2005) 941–950.
[13] G. Hommalai, S.G. Withers, W. Chuenchor, J.R.K. Cairns, J. Svasti, Enzymatic synthesis of cello-oligosaccharides by rice BGlu1 β-glucosidase glycosynthase mutants, Glycobiology 17 (2007) 744–753.
[14] S. Pengthaisong, S.G. Withers, B. Kuaprasert, J. Svasti, J.R. Ketudat Cairns, The role of the oligosaccharide binding cleft of rice BGlu1 in hydrolysis of cellooligosaccharides and in their synthesis by rice BGlu1 glycosynthase, Protein Sci. 21 (2012) 362–372.
[15] J.H. Wang, S. Pengthaisong, J.R.K. Cairns, Y.J. Liu, X-ray crystallography and QM/MM investigation on the oligosaccharide synthesis mechanism of rice BGlu1 glycosynthases, Biochim. Biophys. Acta 1834 (2013) 536–545.
[16] M. Moracci, A. Trincone, M. Rossi, Glycosynthases: new enzymes for oligosaccharide synthesis, J. Mol. Catal. B-Enzym. 11 (2001) 155–163.
[17] J. Noguchi, Y. Hayashi, Y. Baba, N. Okino, M. Kimura, M. Ito, Y. Kakuta, Crystal structure of the covalent intermediate of human cytosolic β-glucosidase, Biochem. Biophys. Res. Commun. 374 (2008) 549–552.
[18] G.M. Morris, D.S. Goodsell, R.S. Halliday, R. Huey, W.E. Hart, R.K. Belew, A.J. Olson, Automated docking using a Lamarckian genetic algorithm and an empirical binding free energy function, J. Comput. Chem. 19 (1998) 1639–1662.
[19] J. Gasteiger, M. Marsili, Iterative partial equalization of orbital electronegativity – a rapid access to atomic charges, Tetrahedron 36 (1980) 3219–3228.
[20] M.A. Marti-Renom, A.C. Stuart, A. Fiser, R. Sanchez, F. Melo, A. Sali, Comparative protein structure modeling of genes and genomes, Annu. Rev. Biophys. Biomol. Struct. 29 (2000) 291–325.
[21] A. Sali, T.L. Blundell, Comparative protein modelling by satisfaction of spatial restraints, J. Mol. Biol. 234 (1993) 779–815.
[22] A. Fiser, R.K. Do, A. Sali, Modeling of loops in protein structures, Protein Sci. 9 (2000) 1753–1773.
[23] H. Li, A.D. Robertson, J.H. Jensen, Very fast empirical prediction and rationalization of protein pKa values, Proteins 61 (2005) 704–721.
[24] D.C. Bas, D.M. Rogers, J.H. Jensen, Very fast prediction and rationalization of pKa values for protein–ligand complexes, Proteins 73 (2008) 765–783.
[25] B.R. Brooks, R.E. Bruccoleri, B.D. Olafson, D.J. States, S. Swaminathan, M. Karplus, CHARMM: a program for macromolecular energy, minimization, and dynamics calculations, J. Comput. Chem. 4 (1983) 187–217.
[26] A.D. MacKerell, D. Bashford, M. Bellott, R. Dunbrack, J. Evanseck, M.J. Field, S. Fischer, J. Gao, H. Guo, S.A. Ha, All-atom empirical potential for molecular modeling and dynamics studies of proteins, J. Phys. Chem. B 102 (1998) 3586–3616.
[27] R. Ahlrichs, M. Bär, M. Häser, H. Horn, C. Kölmel, Electronic structure calculations on workstation computers: the program system turbomole, Chem. Phys. Lett. 162 (1989) 165–169.
[28] W. Smith, T.R. Forester, DL_POLY_2: 0: a general-purpose parallel molecular dynamics simulation package, J. Mol. Graph. 14 (1996) 136–141.
[29] D. Bakowies, W. Thiel, Hybrid models for combined quantum mechanical and molecular mechanical approaches, J. Phys. Chem. 100 (1996) 10580–10594.
[30] A.H. de Vries, P. Sherwood, S.J. Collins, A.M. Rigby, M. Rigutto, G.J. Kramer, Zeolite structure and reactivity by combined quantum-chemical-classical calculations, J. Phys. Chem. B 103 (1999) 6133–6141.
[31] P. Sherwood, A.H. de Vries, M.F. Guest, G. Schreckenbach, C.R.A. Catlow, S.A. French, A.A. Sokol, S.T. Bromley, W. Thiel, A.J. Turner, QUASI: a general purpose

implementation of the QM/MM approach and its application to problems in catalysis, J. Mol. Struct. Theochem. 632 (2003) 1–28.
[32] S.R. Billeter, A.J. Turner, W. Thiel, Linear scaling geometry optimisation and transition state search in hybrid delocalised internal coordinates, Phys. Chem. Chem. Phys. 2 (2000) 2177–2186.
[33] J. Nocedal, Updating quasi-Newton matrices with limited storage, Math. Comput. 35 (1980) 773–782.
[34] D.C. Liu, J. Nocedal, On the limited memory BFGS method for large scale optimization, Math. Program. 45 (1989) 503–528.
[35] A. Banerjee, N. Adams, J. Simons, R. Shepard, Search for stationary points on surfaces, J. Phys. Chem. 89 (1985) 52–57.
[36] J. Baker, An algorithm for the location of transition states, J. Comput. Chem. 7 (1986) 385–395.
[37] W. Chuenchor, S. Pengthaisong, R.C. Robinson, J. Yuvaniyama, J. Svasti, J.R.K. Cairns, The structural basis of oligosaccharide binding by rice BGlu1 beta-glucosidase, J. Struct. Biol. 173 (2011) 169–179.
[38] H.L. Woodcock, M. Hodoscek, B.R. Brooks, Exploring SCC-DFTB paths for mapping QM/MM reaction mechanisms, J. Phys. Chem. A 111 (2007) 5720–5728.
[39] N.F. Brás, S.A. Moura-Tamames, P.A. Fernandes, M.J. Ramos, Mechanistic studies on the formation of glycosidase-substrate and glycosidase-inhibitor covalent intermediates, J. Comput. Chem. 29 (2008) 2565–2574.
[40] A. Ben-David, G. Shoham, Y. Shoham, A universal screening assay for glycosynthases: directed evolution of glycosynthase XynB2(E335G) suggests a general path to enhance activity, Chem. Biol. 15 (2008) 546–551.